Figure S1

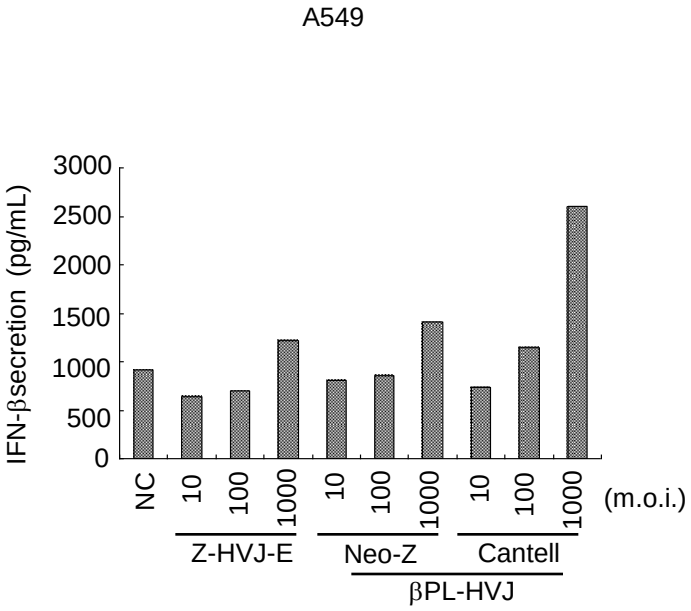

Figure S1. Inactivated-Cantell strain HVJ stimulated IFN-b secretion in A549 cells.
A549 cells were treated with Z-HVJ-E, βPL-Neo-Z and βPL-Cantell strain of HVJ at an m.o.i. of 10-1,000. IFN-β secretion was detected by an ELISA assay 24 hours after A549 cells were treated with inactivated-HVJs (n=2).

Figure S2

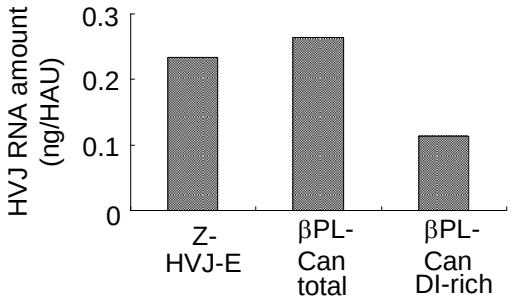

Figure S2. The RNA amount of inactivated-HVJs. HVJ RNAs were isolated from Z-HVJ-E, βPL-Can-total or Can-DI-rich. The RNA concentration of inactivated-HVJ was measured with a spectrophotometer.

Figure S3

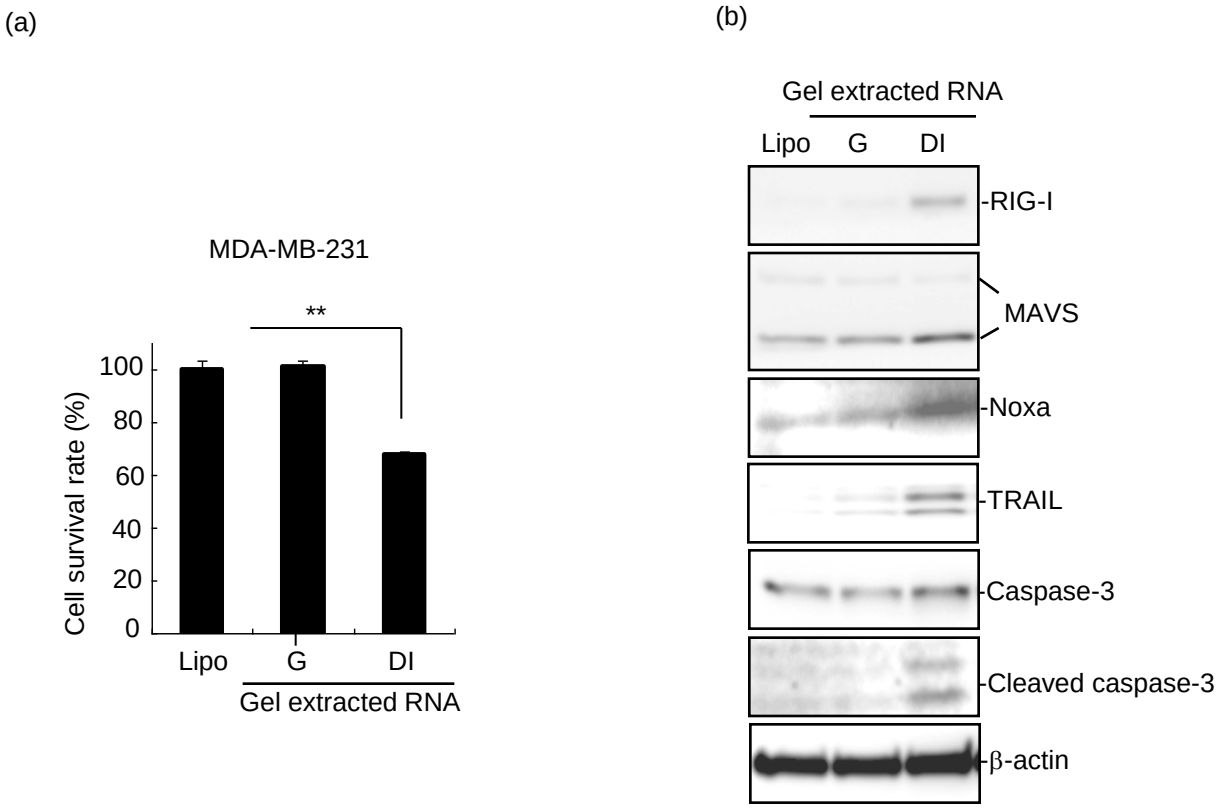

Figure S3. Gel-extracted DI RNA was more efficient than Cantell strain HVJ whole-genome RNA for suppressing MDA-MB-231 cell survival and the induction of apoptosis-related protein expression. HVJ RNA was isolated from βPL-treated Cantell strain HVJ. The Cantell HVJ whole-genome RNA or DI genome RNA was extracted from the agarose gel. (a) The gel-extracted Cantell HVJ whole genome (G) or the DI RNA (DI) (1.33 ng/mL) was transfected into MDA-MB-231 cells. The cell survival was assessed via MTS assay 48 hours after RNA transfection. The mean±SD is shown (n=3). *=significant at $p<0.05$; **=significant at $p<0.01$. (b) Expression levels of RIG-I, MAVS, Noxa, TRAIL and caspase-3 in MDA-MB-231 cells were measured by Western blot analysis 24 hours after RNA (0.133 ng/mL) transfection. “Lipo” indicates cells that were treated with Lipofectamine RNAiMAX without RNA.

Figure S4

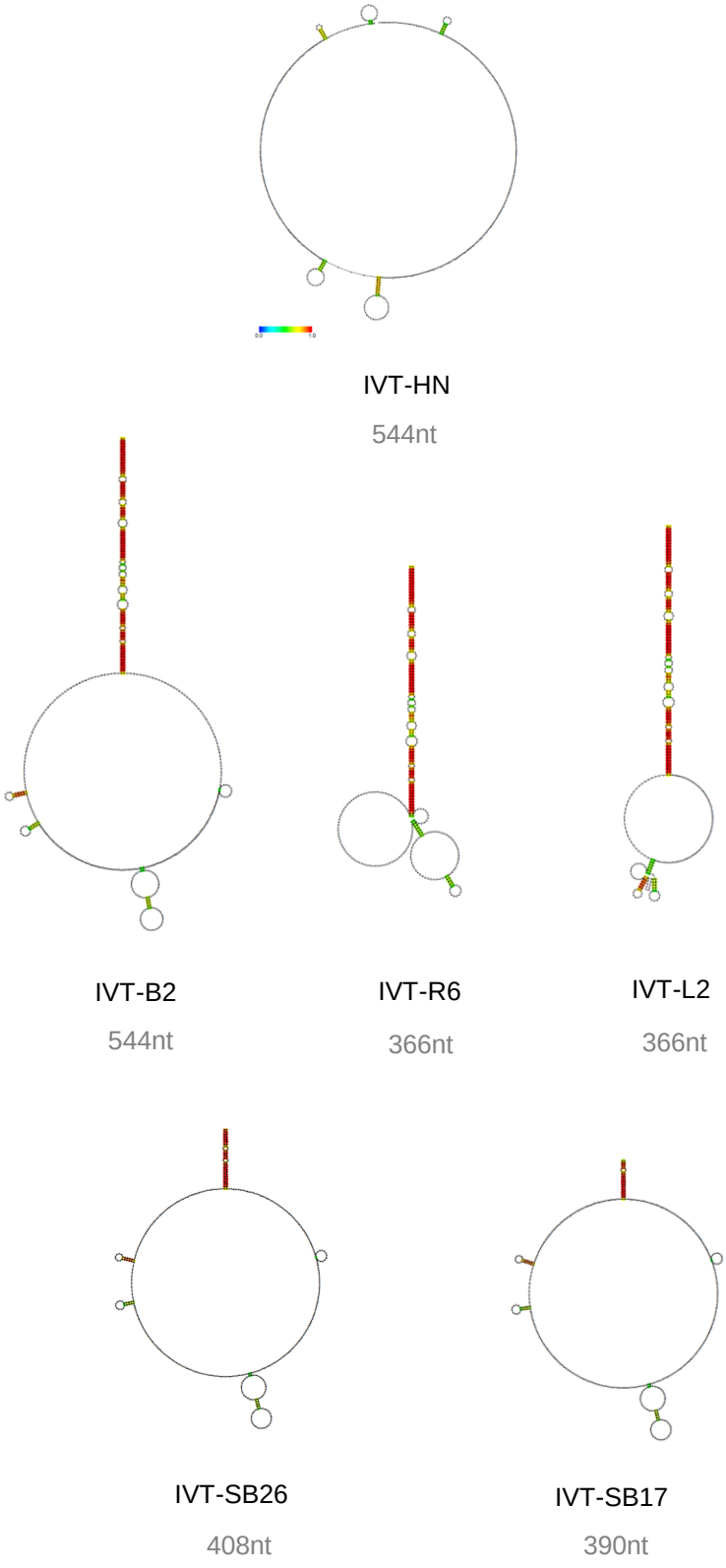

Figure S4. The secondary structure of IVT-RNAs. The secondary structures of IVT-RNAs were predicted according to the RNA sequences by CentroidFold. The heat color gradation from blue to red corresponds to the base-pairing probability of 0 to 1.

Figure S5

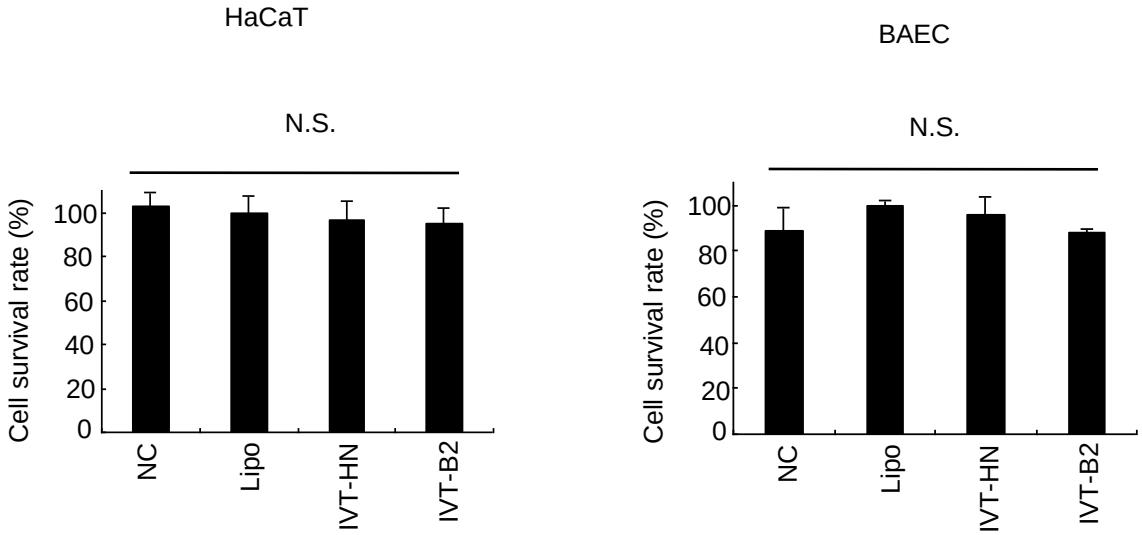

Figure S5. Survival of non-cancerous cells by IVT-B2 transfection The IVT RNAs were transfected into HaCaT and BAEC cells, and the cell survival was detected by MTS assay 48 hours after RNA transfection.

Figure S6

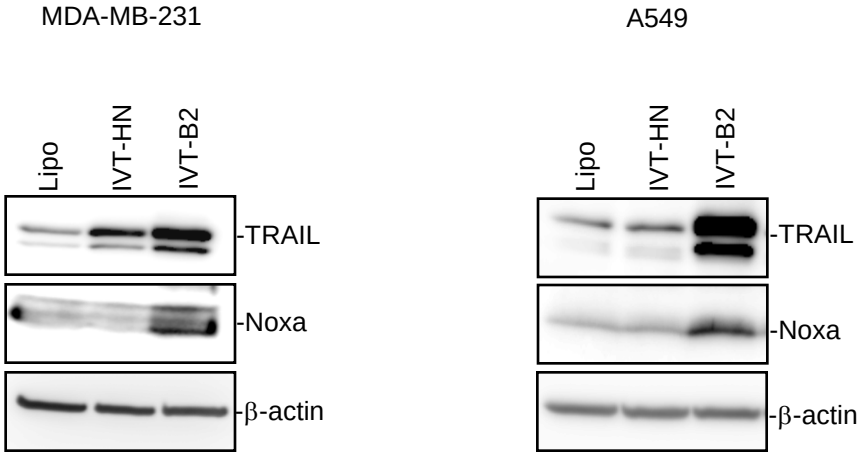

Figure S6. IVT-B2 RNA induced pro-apoptotic protein expression in MDA-MB-231 and A549 cells. Expression levels of Noxa and TRAIL in MDA-MB-231 and A549 cells were measured by Western blot analysis 24 hours after RNA transfection.

Figure S7

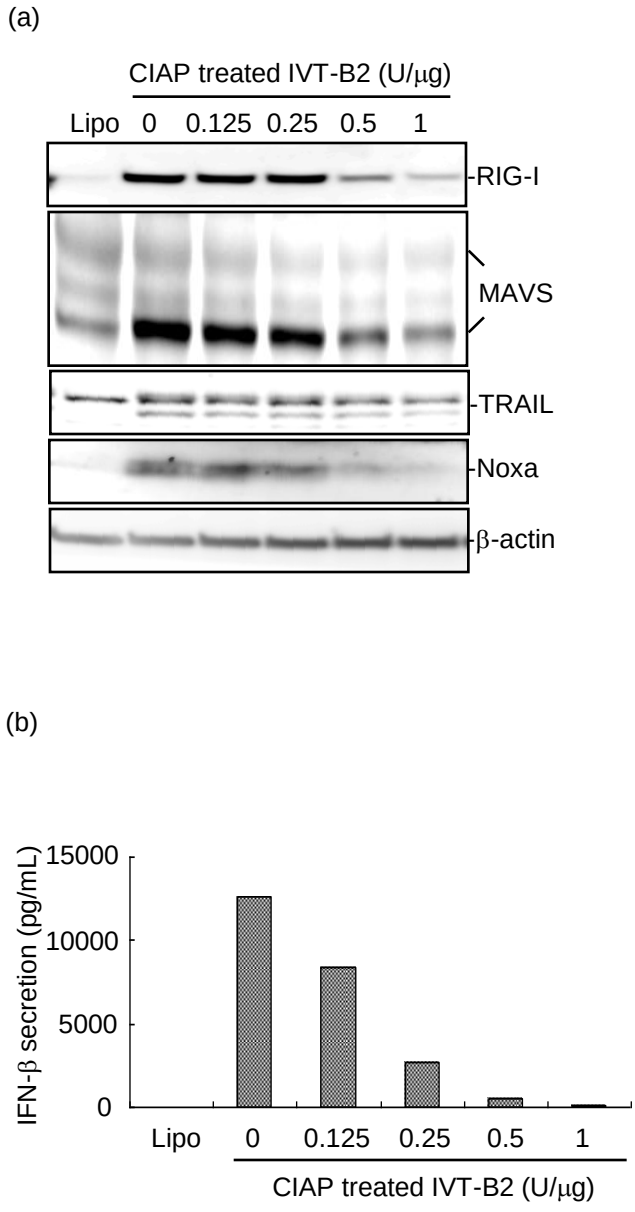

Figure S7. Dephosphorylated IVT-B2 RNA lost the capability of inducing RIG-I/MAVS-related downstream proapoptotic protein expression. (a) The expression of RIG-I, MAVS, Noxa and TRAIL in PC3 cells was assessed by Western blot analysis 24 hours after CIAP-treated IVT-B2 RNA transfection. (b) IFN-β secretion in the culture medium of the PC3 cells was detected by ELISA assay 24 hours after the CIAP-treated IVT-B2 RNA transfection (n=2).

Figure S8

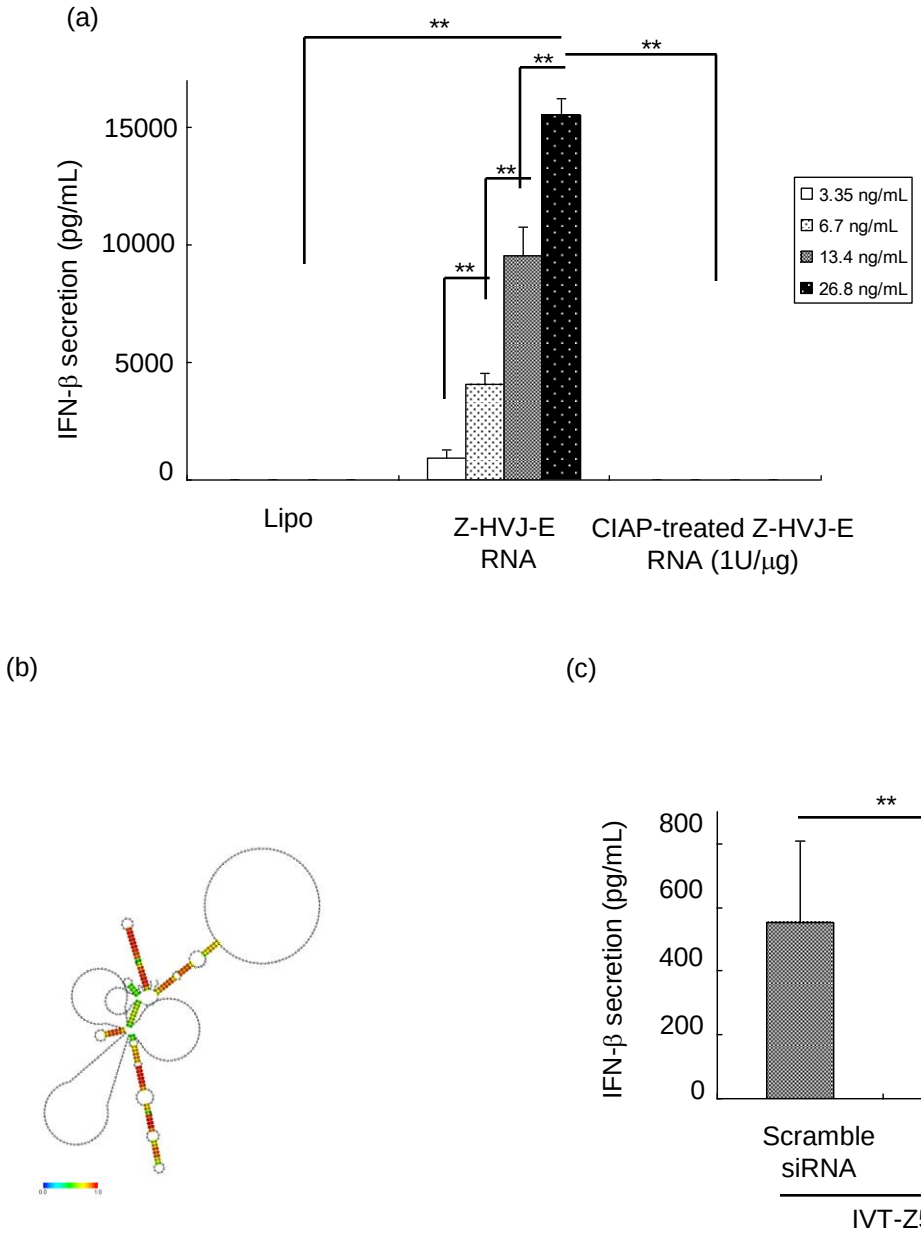

Figure S8. The *in vitro* transcription produced Z strain HVJ genome 5' end RNA (IVT-Z544) induced RIG-I dependent IFN-b secretion in PC3 cells. (a) IFN-β secretion in the culture medium of the PC3 cells was detected by ELISA assay 24 hours after transfection of RNA fragments of UV-inactivated Z strain-HVJ-E or CIAP (1 U/μg)-treated Z-HVJ-E. "Lipo" indicates cells that were treated with Lipofectamine RNAiMAX without RNA. The mean±SD is shown (n=3). (b) The secondary structure of IVT-Z544 was predicted according to the RNA sequences by CentroidFold. The heat color gradation from blue to red corresponds to the base-pairing probability of 0 to 1. (c) IVT-Z544 RNA (1.16 ng/mL) was transfected into RIG-I-knocked-down PC3 cells (RIG-I siRNA) or control PC3 cells (Scramble siRNA). IFN-b secretion was assessed 48 hours after IVT-Z544 RNA transfection. The mean±SD is shown (n=3). **= significant at $p<0.01$.